Environmental Science and Pollution Research (2021) 28:59486–59498
https://doi.org/10.1007/s11356-021-13602-5

RECENT DEVELOPMENTS AND INNOVATIVE STRATEGIES IN ENVIRONMENTAL SCIENCES IN EUROPE

Chemical and morpho-structural characterization of atmospheric aerosol (PM_{10} and $PM_{2.5}$) in a city of São Paulo state, Brazil

Bruno Trevizan Franzin [1,2] · Filipe Corrêa Guizellini [1] · Ossamu Hojo [1] · Iêda Aparecida Pastre [3] · Mary Rosa Rodrigues de Marchi [1] · Hugo Félix Silva [2,4] · Fernando Luis Fertonani [1,3] · Cristina Maria Oliveira [2]

Received: 10 August 2020 / Accepted: 17 March 2021 / Published online: 12 April 2021

Abstract

To access the sources of air pollutants is crucial to control atmospheric pollution in urban areas, minimizing human exposure. Particulate matter is a pollutant of great concern making its chemical and morpho-structural characterization of enormous importance. The present work aims at the characterization of atmospheric PM_{10} and $PM_{2.5}$. Data of the aerosol mass concentration was correlated by multivariate analysis with water-soluble ion fraction composition accessed by ion chromatography (IC), as well as with meteorological information and air mass backward trajectories. The gravimetric analysis presented average values 3 to 4 times higher than the guide values recommended by the World Health Organization (WHO). A morpho-structural analysis by SEM/FEG coupled to EDS was also carried out identifying the coarse fraction elements from minerals and from soil resuspension organic spherical particles that originated from combustion processes as well as Ti, associated with long-distance transportation. In the fine fraction, Zn with origin probably in tires and vehicle brakes was found. These origins were confirmed by the air masses' backward trajectories obtained by the HYSPLIT model (NOAA). This study contributes to a better understanding of the complex composition of the particulate material in the atmosphere of Araraquara City, resulting from the combination of local and long-distance sources, and serves as a basis for the comparison with future studies related to the air quality at this and other regions in Brazil and in the world.

Keywords Urban aerosol · PM_{10} · $PM_{2.5}$ · SEM-EDS · IC

Introduction

Nowadays, it is estimated by the United Nations that the majority of the world population lives in urban areas and about 80% of these urban centers do not reach the air quality standards set by the World Health Organization (UN 2018).

Air pollution is recognized to affect human health (Arbex et al. 2012) and numerous studies conducted in different parts of the world show that the risks of pathologies like respiratory disease (Kim et al. 2018), chronic obstructive pulmonary disease (COPD) (Moore et al. 2016), asthma (Zheng et al. 2015), cardiovascular diseases (Polichetti et al. 2009; Tian et al. 2017), lung cancer (Hamra et al. 2014), and increased risk of diabetes (Reis et al. 2009; Riant et al. 2018; Janjani et al. 2020) are associated with the increasing pollution levels.

Atmospheric contamination by aerosols, the most complex air pollutant, is one of the greatest important environmental problems affecting millions of people, mainly in urban areas of developing countries, with significant impacts on the

Responsible Editor: Gerhard Lammel

✉ Bruno Trevizan Franzin
btfranzin@gmail.com

[1] São Paulo State University (Unesp), Institute of Chemistry, Araraquara, SP 14800-060, Brazil

[2] Centro de Química Estrutural, Faculdade de Ciências, Universidade de Lisboa, Edif. C8, Campo Grande, 1749-016 Lisbon, Portugal

[3] São Paulo State University (Unesp), Biosciences, Languages and Exact Sciences Institute, Ibilce, São José do Rio Preto, SP 15054-000, Brazil

[4] Área Departamental de Engenharia Química do Instituto Superior de Engenharia de Lisboa, ISEL-ADEQ, Rua Conselheiro Emídio Navarro, 1, 1059-007 Lisbon, Portugal

human health and well-being and high economic repercussion. Aerosols are mixtures of particles emitted from natural or anthropogenic sources with different sizes and different chemical compositions (Keuken et al. 2013; Vu et al. 2015).

Pollution caused by $PM_{2.5}$ is mostly associated with particles of anthropogenic origin. In terms of chemical composition, these particles are composed frequently not only of organic pollutants, including volatile organic compounds (VOC) (EPA 2018) and polycyclic aromatic hydrocarbons (PAH) (Oliveira et al. 2011; Callen et al. 2011), but also of metals such as As, Al, Cr, Cu, Fe, Ni, Mn, Pb, Si, Zn, and Pb (Gonçalves et al. 2017; Soleimani et al. 2018), and of water-soluble ionic compounds, whose composition involves typically sulfate (SO_4^{2-}), nitrate (NO_3^-), and chloride (Cl^-) as anions and ammonium (NH_4^+), sodium (Na^+), and calcium (Ca^{2+}) as cations (Mouli et al. 2003; Arias et al. 2013; Kušan et al. 2020).

According to Miranda et al. (2012), in several urban areas of Brazil as in other developing countries, motor vehicles are the major pollution source to be considered. Performing a morpho-structural characterization of particulate matter by electron microscopy high-resolution of field emission gun scanning (SEM-FEG) coupled to energy dispersive spectroscopy (EDS) allows identifying different types of particles and then inferring their probable emission sources (Mico et al. 2015).

HYSPLIT back trajectory model developed by NOAA is an available tool of easy use that permits the identification of pollution sources originating from long distances. When employed associated with principal component analysis (PCA), a tool widely used, it allows an evaluation of correlation between main components of aerosol and their probable sources (Urbančok et al. 2017).

The present work aims to characterize PM_{10} and $PM_{2.5}$ aerosol of a city from the center of São Paulo state, Brazil, in terms of mass by gravimetry, ionic chemical composition by ionic chromatography, and a morpho-structural and elemental analysis through SEM/FEG-EDS. The obtained results were correlated by PCA analysis with meteorological data and air mass trajectories in order to identify the probable emitting sources of the urban atmospheric aerosol sampled in the city. The calculation of enrichment factors (EF) for the most abundant ions present in the samples also contributed to the identification of those probable emitting sources. At the same time, this characterization was used for the verification of the adequacy to the use of the Gent type sampler used in the sampling step and manufactured by the team.

Materials and methods

Sampling

Aerosol sampling was conducted within the Araraquara Campus from the São Paulo State University (UNESP) (21° 80′ 77.54″ S; 48° 19′ 22.50″ W), in a densely populated urban area and very close (about 50 m) to the federal high-traffic highway Washington Luis (Fig. 1). Araraquara is a medium-sized city in São Paulo state, in Brazil, with approximately 250,000 inhabitants and with about 97% of the population living in the urban area. The city located in an agro-industrial region, in the center of São Paulo state, is surrounded by two highways presenting significant motor vehicle traffic.

The sampling campaign, with a total of 104 samples, was carried out from November 09, 2017, to October 10, 2018, passing through all the seasons.

A low-cost Gent type sampler built by the team (Franzin et al. 2021), equipped with an SFU (stacked filter unit) with capacity for two filters, to collect $PM_{10-2.5}$ (coarse fraction) and $PM_{2.5}$ (fine fraction), installed 1.60 m above the soil was used. The complete sampling system consists of a vacuum pump, operating at a flow rate of about 16 L min^{-1} (0.96 m^3 h^{-1}) (Maenhaut et al. 1994; Hopke et al. 1997), a rotameter (for sampled air volume control), and a gas meter in addition to the Gent type sampler.

To collect $PM_{10-2.5}$ and $PM_{2.5}$ polycarbonate, membrane filters Nuclepore™ Track-Etch Membrane from Whatman® with 47 mm diameter and porosities of 8.0 and 0.4 μm, respectively, were used. Filters were manually replaced in 24h sampling periods.

Meteorological data were obtained from the Companhia Ambiental do Estado de São Paulo – CETESB, QUALAR platform (Cetesb 2018).

Gravimetric analysis

Filters were weighed using an analytical balance Mettler Toledo, model AG 245 with resolution of 0.01 mg, placed in a room with controlled relative humidity (50±5) % and temperature (25±2) °C. Filter mass before and after sampling was obtained under repeatability conditions (n > 3), aiming at minimizing the mass uncertainty. The mass concentration of particles was expressed in nanograms per cubic meter of sampled air (ABNT 1997). The exposed filters were cut into two parts (Bettencourt da Silva et al. 2012), stored in PetriSlides™ from Millipore®, properly sealed, and frozen until other analyses were performed. Blank filters were also analyzed, and the blank concentrations were subtracted from the values obtained for each sample.

Aerosol chemical and morphological characterization

Ion chromatography analysis

For ion analyses, blank filters and samples were extracted with 5 mL of ultrapure water (18.4 MΩ cm), 45 min in ultrasonic bath (Branson 3200). The extracts were

Fig. 1 Google Earth™: I, map of Brazil with São Paulo state signed. II, Map of São Paulo state with Araraquara marked. III, Sampling site (yellow pin) with the surroundings and the Washington Luis highway–SP-310 in the map of Araraquara City

filtered through a pre-washed Whatman 41® filter and then analyzed by IC.

Cations were measured in a Dionex® DX500 system with conductivity detection (CD20), equipped with Peaknet® software. The chromatograph was equipped with an isocratic pump IP20, a column guard Ion Pack CG12, an Ion Pack CS12 column, and a CSRS 300-II-4mm cation suppressor. The eluent was methane sulfonic acid 20 mM solution with a flow rate of 1.0 mL min^{-1}. Anions were analyzed in a Metrohn 881 Compact IC pro, equipped with an IC Professional Detector and a chemical suppressor "packed-bed" (H_2SO_4, 100 mmol L^{-1} solution), an anion pre-column IonPack AG14 4×50 mm and an analytical column IonPack AS14 4×250 mm. The eluent was a 3.5 mmol dm^{-3} Na_2CO_3 + 1 mmol dm^{-3} $NaHCO_3$ buffer solution at a flow rate of 1.2 mL min^{-1}. The injection volumes were 100 μL for anions and 25 μL for cations.

Sample analyses were performed after the daily calibration of the chromatograph systems using calibrator mass concentrations fit for the application of the linear regression model confirmed by application of the spreadsheet developed by Bettencourt da Silva (2016).

Five cations (Na^+, NH_4^+, K^+, Mg^{2+}, and Ca^{2+}) and seven anions (F^-, Cl^-, NO_2^-, Br^-, PO_4^{3-}, SO_4^{2-}, and $C_2O_4^{2-}$) were analyzed in 52 $PM_{2.5}$ and 52 $PM_{10–2.5}$ samples.

Electron microscopy high-resolution of field emission gun scanning (SEM/FEG)

The morpho-structural characterization of sampled particles was performed by SEM/FEG-EDS with equipment JEOL model JSM-7500F, equipped with secondary electron and backscattering (BSE) detectors, operating at 10 kV at low vacuum conditions (30 Pa), and PC-SEM v 2.1.0.3 software. Elemental analysis (energy dispersive spectroscopy, EDS) was performed with an Ultra Dry model from Thermo Scientific, with NSS 2.3 operation software. Samples and blanks were prepared by removing a piece of filter equivalent to an area of 0.1 cm^2. Then, each sample piece was coated with a carbon wire under vacuum to increase conductivity (Franzin et al. 2020).

Air mass backward trajectories

To investigate the transport of air pollutants, 96h air mass backward trajectory analyses were conducted using the HYSPLIT model, version 4.0 (www.arl.noaa.gov/HTSPLIT.php) with a starting height of 200 m in the geographic coordinates, 21° 80′ 77.54″ (S), 48° 19′ 22.50″ (W). Trajectories were obtained through the READY platform - *Real-time Environmental Applications* and *Displays* System (Rolph et al. 2017).

Enrichment factors (EF)

To evaluate the crustal and non-crustal origin of the studied compounds, the crustal EF method is still widely used. For the crustal enrichment factor, several reference elements are being reported in the literature such as Si, Al, Fe, Ti, and Sc, of which Al is used in the majority of the studies (Hoornaert et al. 2004).

Enrichment factors, using Al as a crustal reference element (EFAl), were calculated based on Eq. (1) and using Mason and Moore (1982) soil composition.

$$EF\mathrm{Al} = \frac{(C_x/C_{\mathrm{ref}})_{\mathrm{aerosol}}}{(C_x/C_{\mathrm{ref}})_{\mathrm{crust}}} \quad (1)$$

where Cx is the concentration of the element or species under study in the aerosol or in the crust and Cref is the concentration of the reference element in the aerosol or in the crust.

Principal component analysis (PCA)

To evaluate the potential correlation between water-soluble ion fraction composition, particle mass concentrations, and meteorological parameters, a multivariate statistical PCA and hierarchical cluster analysis (HCA), using Statistica 8.0.360 software (Statistica 2007), was performed.

Results and discussion

PM mass concentration

The mass concentration profiles obtained for the fine ($PM_{2.5}$) and coarse (PM_{10}) fractions from the sampling period in the city of Araraquara are shown in Fig. 2.

It can be seen from Fig. 2 that the predominant aerosol mass is in PM_{10} fraction and the mass values in this fraction exceeded 11 times the maximum daily value of 50 μg m^{-3} (red dashed line) recommended by WHO (2006). These exceedances were observed mainly in June–July, corresponding to the driest period of the year with many burnt sugarcane events and consequently the presence of smoke.

For the fine fraction were recorded 10 days of exceedances to the WHO recommended value of 25 μg m^{-3} (blue dashed line), 2 days in November 2017, and 8 days in June–July 2018. In these days, contributions from local sources of pollution were not observed, having been recorded in both periods of dry weather, corresponding to low relative humidity which favors the concentration of pollutants in the atmosphere. In both fractions, daily particle mass concentrations exceeded 3 to 4 times the WHO recommended values.

Monthly averages of meteorological parameters and particle mass concentrations (PM_{10} and $PM_{2.5}$) for the sampling campaign are presented in Table 1.

It can be seen from Table 1 that June and July recorded the highest average particle concentrations with 28.6 and 60.1 μg m^{-3} in June and 42.6 and 70.4 μg m^{-3} in July for $PM_{2.5}$ and PM_{10}, respectively. These two months correspond to a very dry period with absence of raining and low humidity values. The particle mass concentrations for both the fine and coarse fractions presented values 3 to 4 times higher than the annual WHO recommended values of 10 μg m^{-3} and 20 μg m^{-3}, respectively, showing a critical period of pollution.

According to Table 1, the main wind direction was from the east-northeast (ENE) direction, corresponding to wind coming predominantly from the city.

Inorganic characterization

Morphological and elemental analysis by SEM/FEG-EDS

Based on the results obtained by the gravimetric analysis, four filters were selected to be analyzed by SEM/FEG-EDS. The chosen filters were the ones with the highest particle mass July 04 and 17, 2018, for the coarse fraction and November 23, 2017, and July 17, 2018, for the fine fraction. Blank filters were also analyzed to observe the morphological characteristics of their matrix (Franzin et al. 2020).

Figure 3 shows a cluster of particles of the coarse fraction whose morphology was attributed to sources of natural origin. Particles of this nature, resulting from the resuspension of crust material, were attributed to the clay minerals (EDS; Fig. 3 II-B) due to the presence of Al, Si, Fe, and Mg.

A perfectly spherical particle (yellow crosshair A) in the collected sample suggests the presence of elements of anthropogenic origin in the particulate material. Particles with such morphology, with intense signals in the EDS spectrum for C and O (Fig.3 II-A), were attributed to the presence of soot, volatile ash originating from the burning of biomass (Pósfai et al. 2003) and combustion from industrial sources (Micic et al. 2003).

Results shown in Fig. 3 II-B evidence the presence of a combination of natural and anthropogenic sources in the

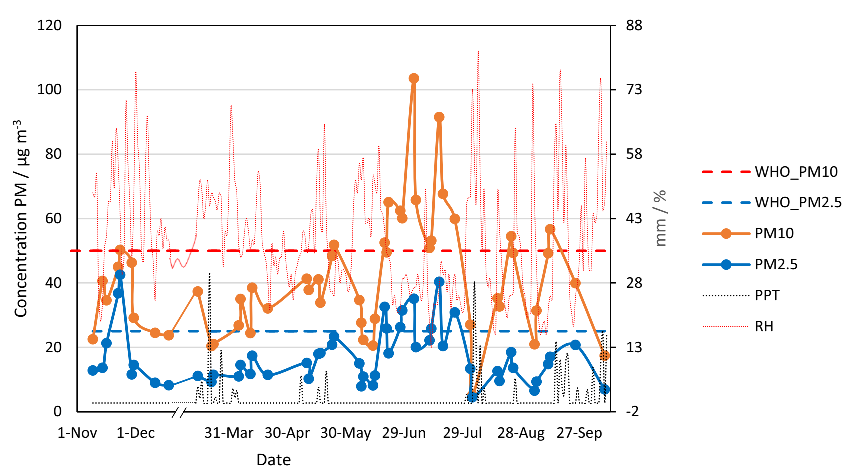

Fig. 2 Aerosol mass profiles: brown, coarse fraction (PM_{10}); blue, fine fraction ($PM_{2.5}$); meteorological data: accumulated precipitation (PPT), relative humidity (RH), and daily maximum values (WHO 2006): dashed red and blue lines

Table 1 Monthly averages of meteorological parameters and particle mass concentrations, PM_{10} and $PM_{2.5}$ ($\mu g\ m^{-3}$), in the sampling period

Month	T (°C)	RH[1] (%)	WS[2] ($m\ s^{-1}$)	WD[3]	PPT[4] (mm)	$PM_{2.5}$ ($\mu g\ m^{-3}$)	PM_{10} ($\mu g\ m^{-3}$)
Nov/2017	30.0	44.5	2.25	NNW	0.0	16.5	38.4
Dec/2017	30.8	44.0	2.05	ENE	0.0	15.5	24.1
Mar/2018	31.1	45.6	2.06	ESE	54.3	15.7	26.3
Apr/2018	28.8	39.5	1.91	ENE	7.50	18.2	31.4
May/2018	27.2	35.8	1.77	ENE	17.5	24.8	42.4
Jun/2018	27.0	39.4	1.82	NE	0.0	28.6	60.1
Jul/2018	27.7	27.1	1.78	ENE	2.00	42.6	70.4
Aug/2018	26.4	37.2	2.05	NE	62.2	22.0	34.0
Sep/2018	28.9	36.3	2.07	ENE	55.1	26.0	39.6
Oct/2018	29.8	47.8	2.25	ESE	54.3	10.5	17.4

[1] Relative humidity

[2] Wind speed

[3] Wind direction

[4] Acummulated precipitation

studied particles. In addition to being from a local natural source (crust), the presence of Ti suggests its occurrence due to the transport of air masses from long distance, which was confirmed from the air mass back trajectories obtained by the HYSPLIT model (Fig. 4). In fact, the air masses arriving to the city in that day passed over the Greater São Paulo region where there are several companies that use compounds containing titanium in the preparation of their products, mainly painting industries.

The EDS analysis in Fig. 3 II-B shows the presence of Al and Si. The probable origin of these elements suggested by the presence of lamellar structures is the soil dust resuspension that can have its origin in agroindustrial activities.

Typically, particles with regular morphology and with a certain degree of symmetry have been related to mineral sources such as soil dust (González et al. 2018), whereas perfectly spherical particles have been related to sources of anthropic origin from high-temperature combustion processes (Satsangi and Yadav 2014).

On what concerns the fine fraction sample, the SEM-FEG image (Fig. 5) shows an agglomerate of particles, as previously observed for the coarse fraction. Point B has morphological characteristics similar to those observed in Fig. 3 and on the correspondent EDS spectrum (Fig. 5 II-B) are present Al, Si, and Fe, elements constituents of aluminosilicates from soil resuspension (Bulbul et al. 2018).

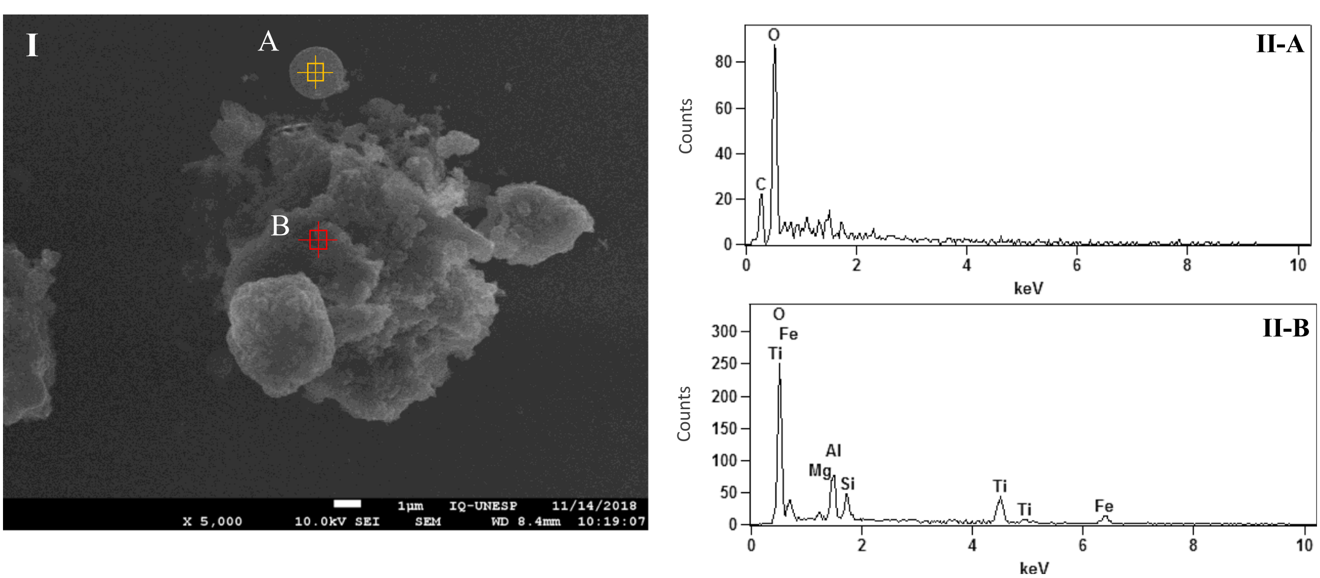

Fig. 3 I, SEM-FEG images of the coarse fraction sample of July 04, 2018; II, EDS spectra regions delimited by the (A) yellow and (B) red crosshair determinations

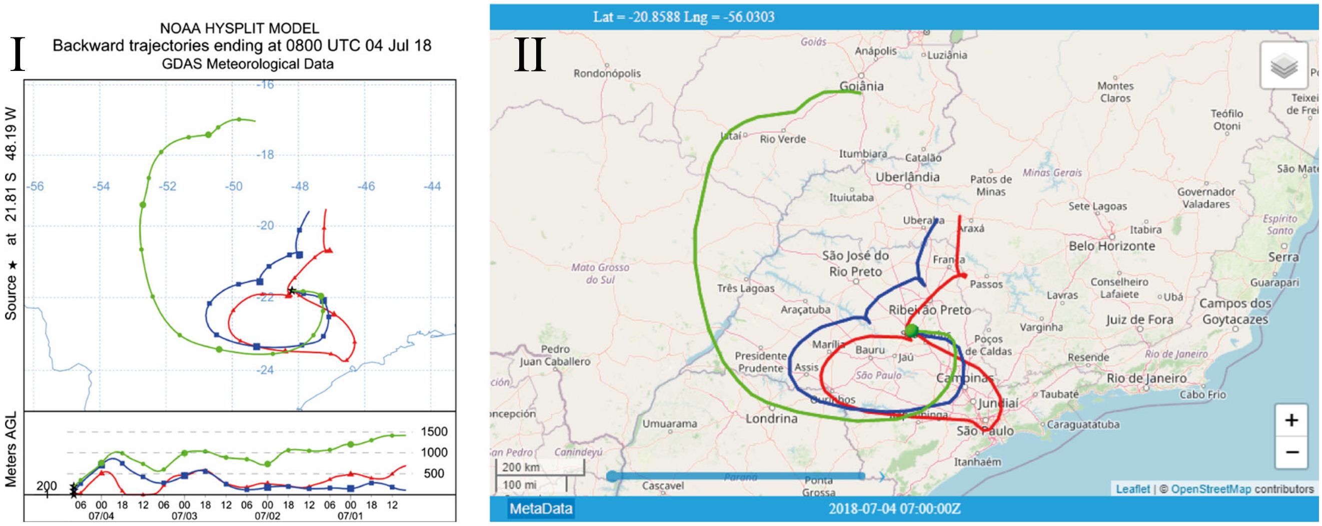

Fig. 4 I, Air mass backward trajectories obtained by the HYSPLIT NOAA model, for July 04 at the sampling site (NOAA 2019). II, The same air mass back trajectories from a satellite perspective taken from Google Earth®

Particle A having a perfectly spherical form is associated to biomass and industrial combustion processes (Satsangi and Yadav 2014; Pósfai et al. 2003; Micic et al. 2003) and the EDS spectrum (Fig. 5 II-A) confirms its anthropogenic origin since, in addition to crustal elements Al, Si, Ca, Fe, and Mg, it also shows Zn and Ti. It should be noted that these spherical particles arising from combustion processes have in general high superficial area and porosity (Chakrabarty et al. 2014; Moallemi et al. 2019) which facilitate the association of elements from different origins, as can be seen in Fig. 5 II-A. Being Zn an indicator of tires and brake wear of vehicles (Grigoratos and Martini 2015), its presence can be associated to the traffic on the highway next to the sampling site and can potentially also have a contribution from non-local sources since air masses obtained for that day passed through the industrialized region of Ribeirão Preto, Franca, and Porto Ferreira, known in the sugar-alcohol, ceramics, and footwear sectors, respectively. The origin of Ti can be attributed to several painting companies that surround the sampling site, which perform electrostatic and liquid painting services (West et al. 2018)

On the SEM-FEG image of Fig. 6, two particles signed with A and B crosshairs are present. A being a particle with a mix of mineral and anthropogenic origins, as observed by the elements Mg, Al, Si, Fe, K, and P, S present in the EDS spectrum of Fig. 6 II-A probably arises from agriculture activities and the use of fertilizers. B represents an amorphous structure, probably a mix of black carbon particles from

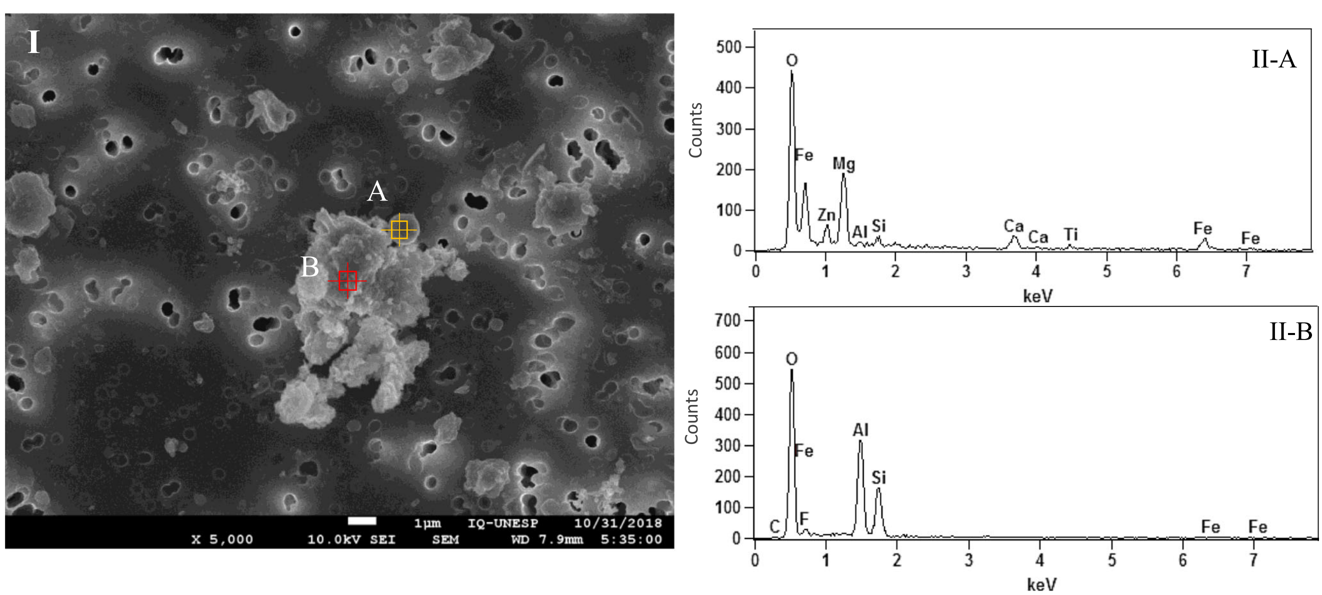

Fig. 5 I, SEM-FEG images of the fine fraction sample of July 17, 2018; II, EDS, regions delimited by the (A) yellow and (B) red crosshair determinations

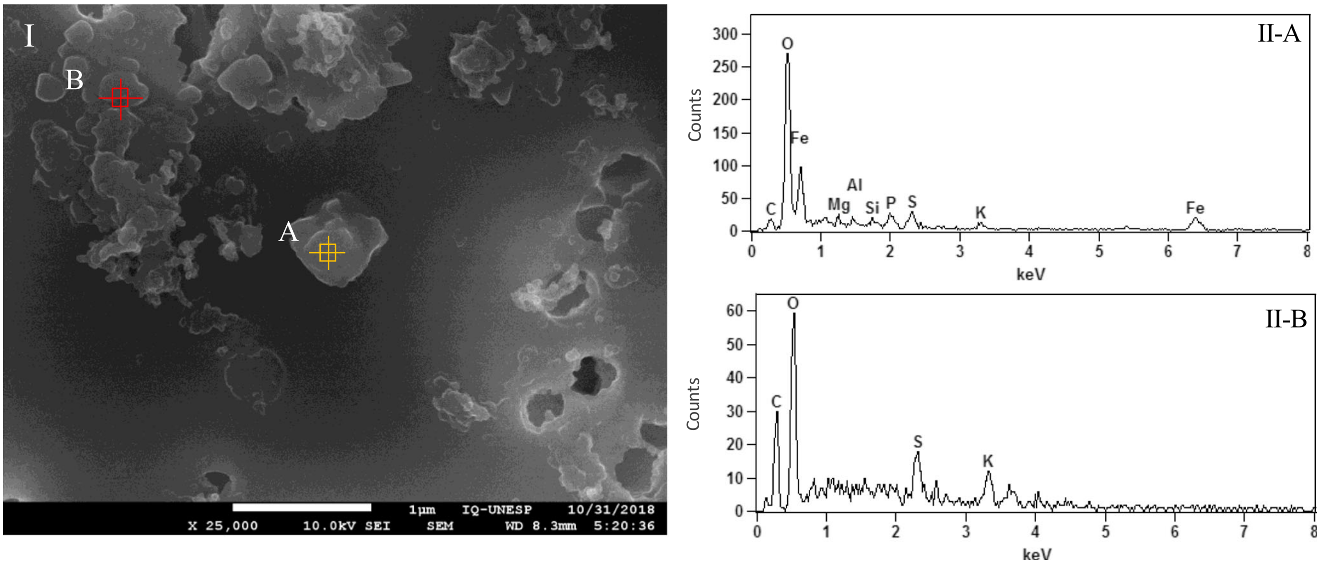

Fig. 6 I, SEM-FEG images of the fine fraction sample of November 23, 2017; II, EDS, regions delimited by the (A) yellow and (B) red crosshair determinations

biomass combustion as suggested by the EDS spectrum (Fig. 6 II-B).

The presence of black carbon, in the fine fraction ($PM_{2.5}$), is associated to hazardous substances to human and animal life as well as to climate changes due to albedo (Twomey 1977; Myhre et al. 2013; Bond et al. 2013; Wiedensohler et al. 2018).

Chemical analysis by ion chromatography

Table 2 presents a statistical summary of the results of cation mass concentrations in the coarse ($PM_{10-2.5}$) and fine ($PM_{2.5}$) fractions. Regarding the average concentrations, cations were present in the aerosol in the following orders $K^+ \geq Ca^{2+} > Na^+ > NH_4^+ > Mg^{2+}$ and $K^+ > NH_4^+ > Ca^{2+} > Na^+ > Mg^{2+}$, for the coarse and the fine fractions, respectively.

The temporal mass concentration profiles of the five cations in the aerosol coarse fraction ($PM_{10-2.5}$) allow observing low concentrations in several days coinciding all with rainy days (Fig. 1S in supplementary material).

A good correlation is observed between K^+ and NH_4^+, $R^2 >$ 0.43. This last ion has in general an anthropogenic origin emitted by the soil in agricultural crops or generated during industrial processes and burning fossil fuels (Sutton et al. 2013).

Although Ca^{2+} presents an average concentration very close to that of K^+, as evidenced by the comparative daily profile of both (Fig. 7 I), the only good correlation observed was with Mg^{2+}, $R^2 > 0.72$ (Fig. 7 II). This result indicates the probable compatibility of sources for calcium and magnesium ions which are notably of mineral origin with a combination of natural (e.g., soil resuspension) and anthropic sources (e.g., application of fertilizers and soil management).

Regarding the fine fraction, of which the temporal mass concentration profiles are presented in Fig. 2S, the most abundant cations are K^+ and NH_4^+ and the only observed correlation was between Na^+ and Ca^{2+} although with a low value, $R^2 > 0.29$. Both ions can have mineral or anthropogenic origins arising from local (soil management or agriculture activities) or long-distance (marine) sources. In fact, in the days corresponding to the higher sodium concentrations, the air masses arriving at the sampling site came from or passed through the Atlantic Ocean (Fig. 8).

The best correlation observed for ammonium ion was with sulfate ($R^2 = 0.37$); and although with a low value, it can probably be due to the use of ammonium sulfate as fertilizer in agriculture activities important in the Araraquara region such as sugarcane or corn (Franco et al. 2008; Silva et al. 2015).

Concerning the analysis of anions, the average mass concentration of the ions (Figs. 3S and 4S) followed the orders $NO_3^- > SO_4^{2-} > C_2O_4^{2-} > Cl^- > PO_4^{3-} > F^- > NO_2^- > Br^-$ and $SO_4^{2-} > NO_3^- > C_2O_4^{2-} > Cl^- > PO_4^{3-} > F^- > NO_2^- > Br^-$ for the coarse ($PM_{10-2.5}$) and the fine ($PM_{2.5}$) fractions, respectively (Table 3).

In the coarse fraction, most anions did not present good correlations between them. However, the pair nitrate-sulfate presents $R^2 > 0.41$, the chloride-sulfate and chloride-fluoride $R^2 > 0.54$ and $R^2 > 0.58$ respectively, and the oxalate has its best correlations with sulfate $R^2 = 0.37$ and chloride $R^2 = 0.36$.

In general, it is possible to state that sulfate, nitrate, and chloride have correlations with each other regarding the emission sources with sulfate and nitrate probably originating from the soil management (use of fertilizers) and chloride from the soil resuspension. These results agree with those obtained in the morpho-structural characterization by MEV/FEG-EDS.

Table 2 Statistical summary of the average cation mass concentration (μg m^{-3}) in the coarse ($PM_{10-2.5}$) and fine ($PM_{2.5}$) fractions

	Cation mass concentration (μg m^{-3})									
	Coarse fraction ($PM_{10-2.5}$)					Fine fraction ($PM_{2.5}$)				
Cations	Na^+	NH_4^+	K^+	Mg^{2+}	Ca^{2+}	Na^+	NH_4^+	K^+	Mg^{2+}	Ca^{2+}
C_{Mean}	0.0914	0.0907	0.1868	0.0364	0.1827	0.0747	0.3292	0.3394	0.0332	0.0895
SD	0.0863	0.0761	0.1643	0.0267	0.1575	0.0458	0.3238	0.2129	0.0418	0.0726
CV %	94%	84%	88%	73%	86%	61%	98%	63%	126%	81%
Maximum	0.3558	0.3922	0.8229	0.1311	0.8996	0.1978	1.9337	1.1513	0.2131	0.3282
Minimum	0.0074	0.0033	0.0104	0.0036	0.0014	0.0077	0.0026	0.0225	0.0008	0.0041

Oxalate presents weak correlations with sulfate and chloride suggesting the existence of a combination of several contributions to its origin, since according to Strzelec et al. (2020) and Klopper et al. (2020), it can have several sources including motor vehicle emission, biomass burning, and oxidation of acetone and ethylene in the atmosphere. On the other hand, it can be considered that the existence of secondary sources of oxalate with possible aggregation in major particles explains the mass concentration values obtained for this ion in the coarse fraction (Kerminen et al. 2000; Yao et al. 2004).

The correlations between the three major anions (nitrate, sulfate, and oxalate) and the gases NOx, NO_2, and O_3 were also evaluated, all of them presenting values of $R^2 < 0.4$. The PCA analysis below brings a contribution to this discussion.

On the fine fraction, the anions show small correlations between each other. The best correlation was observed for the pair chloride-fluoride (R^2=0.61). In addition to the local mineral sources, it is expected that on June 07 these ions had marine origin (a long-distance source) as both presented a big concentration peak. Supporting this assumption is the fact that on that day the air masses came from the ocean (Fig. 8 (a)).

Sulfate was the most abundant anion in the fine fraction and can be linked to two different origins. One is the secondary aerosol, through reaction of the precursor gas SO_2 from the vehicular transportation, industrial combustion processes, among others. The other agriculture activities are connected to the use of fertilizers, namely ammonium sulfate as previously mentioned for the coarse fraction and corroborated by the MEV-FEG-EDS results.

Nitrate presented a mass concentration about three times lower than that of sulfate and it only correlates with oxalate and NOx, in the same order of magnitude (R^2=0.22) which was corroborated by the PCA analysis (Fig. 9 II). These results indicate that one of the possible origins of nitrate is in secondary aerosol (Seinfeld and Pannis 1998; Allen et al. 2004).

Oxalate showed correlation with NOx and NO_2 (R^2~0.40) corroborated by the one presented in the PCA analysis, which can correspond to a contribution of secondary aerosol for the fine fraction of the aerosol in Araraquara.

Enrichment factors

Enrichment factors using Al as a crustal reference element (EFAl) were calculated through Eq. (1) for the ions with higher concentration and are presented in Fig. 9.

EF values higher than 4, observed in the coarse fraction for K^+, Ca^{2+}, Na^+, and Cl^- suggest, according to Duce et al. (1976), strong anthropogenic contribution being probably associated with a resuspension origin. In the fine fraction, that value was only reached for K^+ and Cl^-, probably both associated to resuspension soil from agricultural activities, a main economic activity in the region.

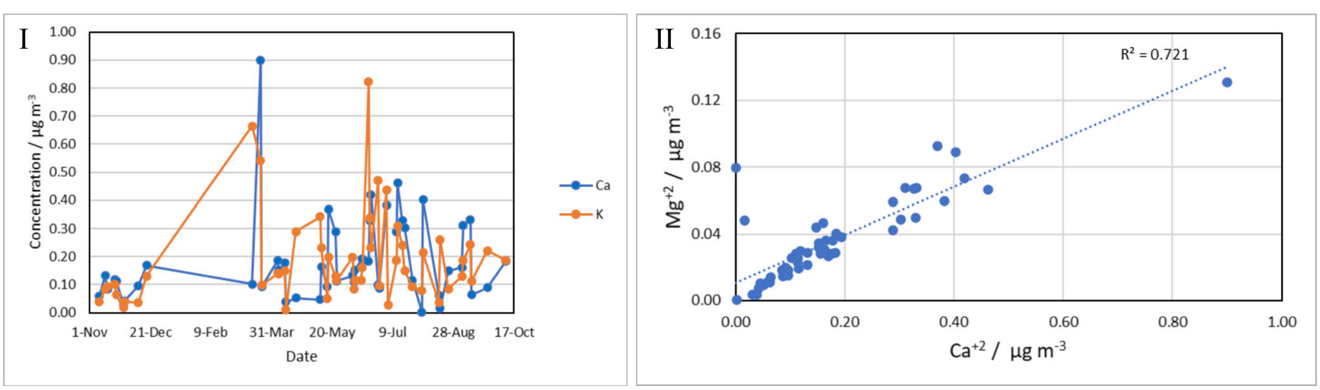

Fig. 7 I, Daily profile of Ca^{2+} and K^+; II, correlation of Ca^{2+} and Mg^{2+} mass concentrations in the coarse fraction

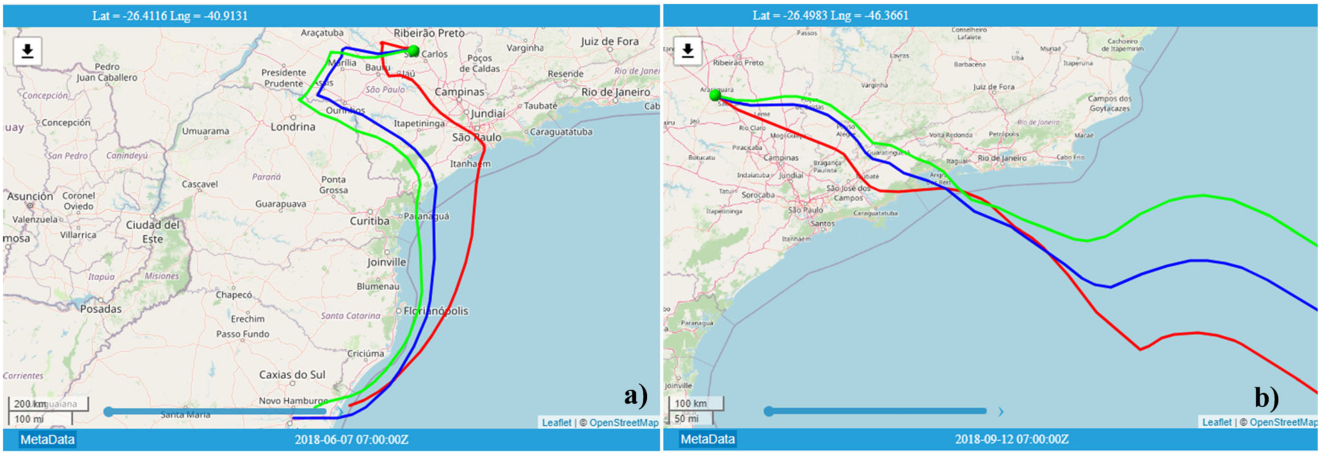

Fig. 8 Air mass back trajectories obtained by the HYSPLIT NOAA model for June 07 (**a**) and September 12 (**b**) 2018, arriving at the sampling site (NOAA 2019). Satellite perspective view taken from Google Earth®

PCA analysis

The PCA graphs of the meteorological data and aerosol precursor gases, both obtained from the QUALAR platform (Cetesb 2018) and the data on the water-soluble composition of $PM_{10-2.5}$ and $PM_{2.5}$ fractions, are shown in Fig. 10 I and II, respectively.

The analysis of these figures reveals the dissimilarity with the main meteorological parameters, precipitation (PPT), relative humidity (RH), wind direction (WD), and temperature (T), being distributed between the 1st and the 4th quadrants as expected and already discussed for the results of gravimetric analysis. The gas components presenting the lowest correlation with the ionic fraction were ozone (O_3), in the 4th quadrant for both fractions, and NO_x and NO_2 in the 3rd, showing similar correlations.

In the 2nd and 3rd quadrants of Fig. 10 I, correlations between the different ions of the coarse fraction can be observed. In the 2nd quadrant, an acute angle (Cruz et al. 2019) is observed between F^- and Cl^- (that presented a 2D correlation of R^2=0.58). Also between NO_3^-, NO_2, and oxalate, correlation is observed, which may indicate the similarity of their emission sources as well as the secondary formation of the ions with the participation of NO_2. This fact can be evidenced by their good correlation with SO_4^{2-}. These correlations corroborate the results obtained by the 2D correlation analyses between these components with R^2 of 0.4 and 0.5.

In the 3rd quadrant of Fig. 10 I are essentially cations with the exception for NO_2^- and PO_4^{3-} anions and NO_x gas. Nitrite and NO_x show good correlation, indicating as probable source of nitrite secondary particulate material since NO_2^- did not show 2D correlation with any ionic component.

The cations present in the 3rd quadrant (Fig. 10 I) confirm the interrelationships with each other already observed by the 2D correlations between K^+ and NH_4^+ and Mg^{2+} and Ca^{2+}. Na^+, although having correlation with other components, is

Table 3 Statistical summary of the average anion mass concentration (μg m^{-3}) in the coarse ($PM_{10-2.5}$) and fine ($PM_{2.5}$) fractions

Anions mass concentration (μg m^{-3})	F^-	Cl^-	NO_2^-	Br^-	NO_3^-	PO_4^{3-}	SO_4^{2-}	$C_2O_4^{2-}$
Coarse fraction ($PM_{10-2.5}$)								
Mean	0.0308	0.0827	0.0137	0.0075	0.4807	0.0735	0.3612	0.0864
SD	0.0465	0.0665	0.0103	0.0130	0.2891	0.1062	0.2445	0.0654
CV	151%	80%	75%	173%	60%	144%	68%	76%
Maximum	0.2912	0.4248	0.0541	0.0879	1.2503	0.6030	1.3269	0.2495
Minimum	0.0033	0.0123	< LOD	< LOD	0.0159	0.0064	0.0373	0.0083
Fine fraction ($PM_{2.5}$)								
Mean	0.0392	0.0610	0.0144	0.0051	0.2827	0.0540	0.9873	0.1356
SD	0.0329	0.0381	0.0094	0.0039	0.2271	0.0594	0.5475	0.0715
CV	84%	63%	66%	77%	80%	110%	55%	53%
Maximum	0.2217	0.2524	0.0498	0.0217	0.9590	0.4270	2.5540	0.3970
Minimum	0.0032	0.0153	< LOD	< LOD	0.0591	0.0154	0.0230	< LOD

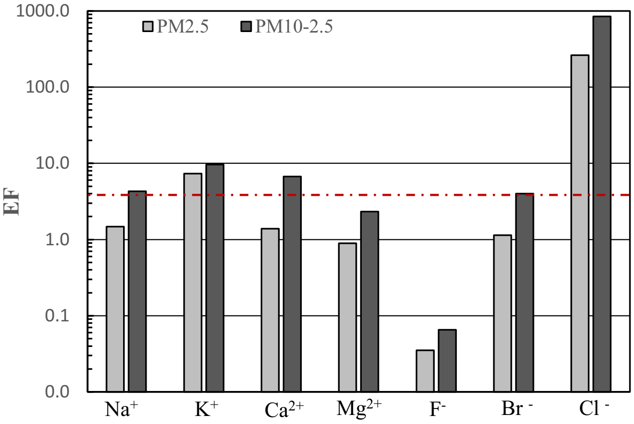

Fig. 9 Average crustal enrichment factors (EF) for different analyzed ions in the coarse and fine fractions, with Al as the reference element. Red dashed line: threshold for anthropogenic contribution (EF=4)

not specifically associated with any of them. Evaluating the PCA graph of the $PM_{2.5}$ fraction, Fig. 10 II, based on the analysis of the 2nd quadrant which presents most components, the correlations stand out between:

1. SO_4^{2-} and NH_4^+ as observed for the 2D correlation, probably arising from the combination of the use of $(NH_4)_2SO_4$ fertilizer and the formation of secondary aerosols by acid-base reactions in the atmosphere,
2. SO_4^{2-} and K^+ corroborating the results obtained by MEV-FEG-EDS, which showed crystals probably of K_2SO_4,
3. K^+ and Mg^{2+} that may indicate their mineral source as reported in the SEM-FEG-EDS results, namely in Fig. 6 II-A,
4. F^-, Na^+, and Cl^- that may have local mineral and oceanic origins, as previously discussed according to the air mass trajectories. Cl^- and F^- have already shown good 2D correlation, $R^2 = 0.61$.
5. NO_3^- and Ca^{2+} that may indicate the predominance of mineral sources linked mainly to the soil and its handling,
6. $C_2O_4^{2-}$ and Ca^{2+} suggesting the contribution from crustal sources by biogenic production combined with secondary formation.

The 3rd quadrant of Fig. 10 II presents the other components and a good correlation between NO_x and NO_2^- that was not observed by the 2D analysis. This result can support their formation by secondary mechanisms probably originating from vehicular emissions, considering the proximity of the Washington Luis - SP-310 highway.

The observed correlation between Br^- and NO_2 in the same quadrant could be explained considering that their low concentrations observed for most days suggest that their main sources are not of local level but probably of long distance, transported by air masses passing through polluted regions, such as Baixada Santista (coast and region of Santos, SP), metropolitan region of São Paulo City, among others, with an appreciable concentration of NO_2 gas.

Conclusions

The results of this work allowed highlighting the possible sources, through the elucidation of the elemental composition and structural morphological analysis, of the particulate matter present in the atmosphere of Araraquara City from November 09, 2017, to October 10, 2018.

The mean mass concentration obtained for PM_{10} and $PM_{2.5}$ fractions presented values almost twice the annual limits recommended by the WHO.

Through a multivariate analysis (PCA, HCA), a correlation of the results from the particle mass concentration ($PM_{10-2.5}$ and $PM_{2.5}$), aerosol ionic composition (IC), and meteorological data, with air mass trajectories (HYSPLIT model) and structural morphological characterization (SEM-FEG), was obtained, confirming the complex composition of atmospheric aerosol in Araraquara City. That composition includes

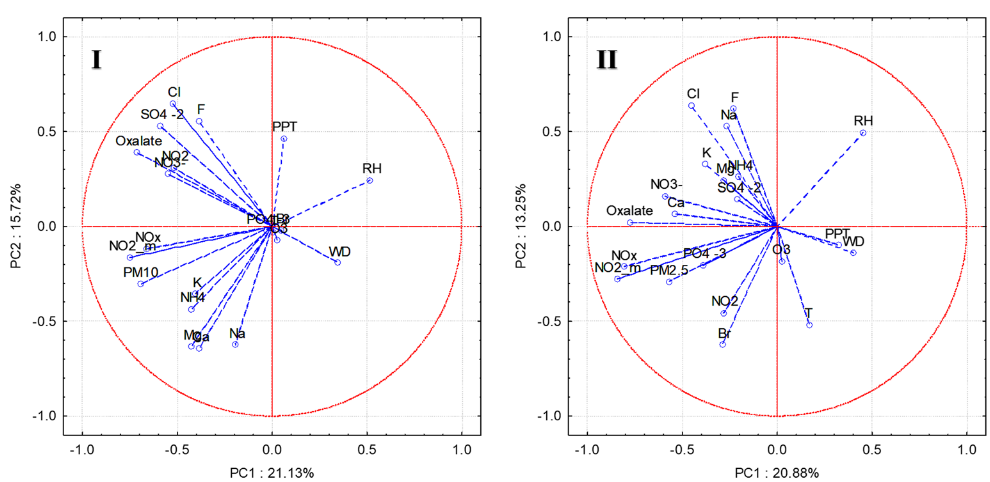

Fig. 10 PCA correlation of water-soluble fraction with meteorological data and precursor gases concentration: I, coarse ($PM_{10-2.5}$); II, fine ($PM_{2.5}$) fractions

particles from both natural and anthropic origins and combines components from local and from long-distances sources, having titanium as the main marker.

The natural sources were identified by elements (Mg, Na, K, Ca) characteristic of the crustal that included clay minerals (Al, Si, Fe), whereas the anthropic ones included agroindustry activities (P and S), biomass burning (K, Cl, C, and O), and vehicular emission, mainly diesel-powered vehicles (S, C, and O), with black carbon as the major component.

The results of this characterization also allow verifying the adequacy to the use of the Gent type sampler used in the sampling step, manufactured by this team, and described in another publication.

Supplementary Information The online version contains supplementary material available at https://doi.org/10.1007/s11356-021-13602-5.

Acknowledgements The authors wish to acknowledge the Scanning and Double Beam Electronic Microscopy laboratory, at the Center for Characterization and Development of Protocols for Nanotechnology (CCDPN-SisNano), Institute of Chemistry, IQ-UNESP, by the FEG-SEM-EDS analysis.

Availability of data and materials The data generated or analyzed during this study are included in this published article or are available from the corresponding author on reasonable request.

Author contribution Conceptualization: BTF, OH, CMO, FLF. Methodology: BTF, OH, MRRM, IAP. Formal analysis and investigation: BTF, OH, FCG, CMO. Writing - original draft preparation: BTF, CMO. Writing - review and editing: BTF, CMO, FCG, HFS. Funding acquisition: BTF, CMO, FLF, MRRM. Resources: OH, MRRM, FLF. Supervision: FLF, OH, MRRM, CMO

Funding Coordenação de Aperfeiçoamento de Pessoal de Nível Superior (001); Fundação para a Ciência e Tecnologia, project (UID/QUI/00100/2019).

Declarations

Ethical Approval Not applicable

Consent to publish Not applicable

Consent to participate Not applicable

Conflict of interest The authors declare no competing interests.

References

ABNT – Associação Brasileira de Normas Técnicas (1997) ABNT-NBR-9547: Material particulado em suspensão no ar ambiente – Determinação de concentração total pelo método do amostrador de grande volume. Rio de Janeiro, p 14

Allen AG, Cardoso AA, Rocha GO (2004) Influence of sugar-cane burning on aerosol soluble ion composition in Southeastern Brasil. Atmos Environ 38(30):5025–5038

Arbex MA, de Paula SU, Martins LC, Saldiva PH, Pereira LA, Braga AL (2012) Air pollution and the respiratory system. J Bras Pneumol 38(5):643–655. https://doi.org/10.1590/S1806-37132012000500015

Arias A, Silva RJNB, Camões MFG, Oliveira CMR (2013) Evaluation of the performance of the determination of anions in the water soluble fraction of atmospheric aerosols. Talanta 104:10–16. https://doi.org/10.1016/j.talanta.2012.11.024

Bettencourt da Silva RJN (2016) Spreadsheet for designing valid least-squares calibrations: a tutorial. Talanta 148:177–190. https://doi.org/10.1016/j.talanta.2015.10.0722015.10.072

Bettencourt da Silva RJNB, Arias A, Oliveira CMRR, Camões MF (2012) Assessment of the determination of water-soluble ionic composition of atmospheric aerosols from the analysis of crossed halves of filters. Accred Qual Assur 17:147–157. https://doi.org/10.1007/s00769-012-0889-z

Bond TC, Doherty SJ, Fahey DW, Forster PM, Berntsen T, DeAngelo BJ, Flanner MG, Ghan S, Karcher B, Koch D, Kinne S, Kondo Y, Quinn PK, Sarofim MC, Schultz MG, Schulz M, Venkataraman C, Zhang H, Zhang S, Bellouin N, Guttikunda SK, Hopke PK, Jacobson MZ, Kaiser JW, Klimont Z, Lohmann U, Schwarz JP, Shindell D, Storelvmo T, Warren SG, Zender CS (2013) Bounding the role of black carbon in the climate system: a scientific assessment. J Geophys Res Atmos 118(11):5380–5552. https://doi.org/10.1002/jgrd.50171

Bulbul G, Shahid I, Chishtie F, Shahid MZ, Hundal RA, Zahra F, Shahzad MI (2018) PM10 Sampling and AOD trends during 2016 winter fog season in the Islamabad region. Aerosol Air Qual Res 18:188–199. https://doi.org/10.4209/aaqr.2017.01.0014

Callen MS, Lopez JM, Mastral AM (2011) Characterization of PM10-bound polycyclic aromatic hydrocarbons in the ambient air of Spanish urban and rural areas. J Environ Monit 13:319–327. https://doi.org/10.1039/c0em00425a

Cetesb (2018) - Companhia Ambiental do Estado de São Paulo - QUALAR - Sistema de informações da qualidade do ar. http://qualar.cetesb.sp.gov.br/qualar/home.do Acessed: January 30, 2020.

Chakrabarty RK, Beres ND, Moosmuller H, China S, Mazzoleni C, Dubey MK, Liu L, Mishchenko MI (2014) Soot superaggregates from flaming wildfires and their direct radiative forcing. Sci Rep 4:5508. https://doi.org/10.1038/srep05508

Cruz LPS, Mota ER, Campos VP, Santana FO, Luza SR, Santos DF (2019) Inorganic and organic acids in the atmosphere of the urban area of the city of Salvador, Brazil. J Braz Chem Soc 30:904–914. https://doi.org/10.2157/0103-5053.20180227

Duce R, Hoffman G, Ray B, Fletcher I, Wallace G, Fasching J, Piotrowicz S, Walsh P, Hoffman E, Miller J, Heffter J (1976) Trace metals in the marine atmosphere: sources and fluxes. In: Windom H, Duce R (eds) Marine pollution transfer. Lexington Books, Lexington

Franco HCJ, Trivelin PCO, Faroni CE, Vitti AC, Otto R (2008) Aproveitamento pela cana-de-açúcar da adubação nitrogenada de plantio. Rev Bras Ciênc Solo 32:2763–2770

Franzin BT, Guizellini FC, de Babos DV, Hojo O, Pastre IA, Marchi MRR, Fertonani FL, Oliveira CMRR (2020) Characterization of atmospheric aerosol (PM10 and PM2.5) from a medium sized city in São Paulo state, Brazil. J Environ 89:238–251. https://doi.org/10.1016/j.jes.2019.09.014

Franzin BT, Hojo O, Ferreira MR, Forti MC, Meneghetti CD, Marchi MRR, Oliveira CMRR, Fertonani FL (2021) Low-cost Gent type sampler constructed for urban atmospheric aerosol sampling. Environ Sci Pollut Res. https://doi.org/10.1007/s11356-020-12103-1

Gonçalves C, Figueiredo BR, Alves CA, Cardoso AA, Vicente AM (2017) Size-segregated aerosol chemical composition from an agro-industrial region of São Paulo state, Brazil. Air Qual Atmos Health 10:483–496. https://doi.org/10.1007/s11869-016-0441-0

González LT, Longoria-Rodríguez FE, Sánchez-Domínguez M, Leyva-Porras C, Acuña-Askar K, Kharissov BI, Arizpe-Zapata A, Alfaro-Barbosa JM (2018) Seasonal variation and chemical composition of particulate matter: a study by XPS, ICP-AES and sequential microanalysis using 553 Raman with SEM/EDS. J Environ Sci 74:32–49. https://doi.org/10.1016/j.jes.2018.02.002

Grigoratos T, Martini G (2015) Brake wear particle emissions: a review. Environ Sci Pollut Res 22:2491–2504. https://doi.org/10.1007/s11356-014-3696-8

Hamra GB, Guha N, Cohen A, Laden F, Raaschou-Nielsen O, Samet JM, Vineis P, Forastiere F, Saldiva P, Yorifuji T, Loomis D (2014) Outdoor particulate matter exposure and lung cancer: a systematic review and meta-analysis. Environ Health Perspect 122:906–912. https://doi.org/10.1289/ehp/1408092

Hoornaert S, Godoi RHM, Van Grieken R (2004) Elemental and single particle aerosol characterisation at a background station in Kazakhstan. J Atmos Chem 48:301–315

Hopke PK, Xie Y, Raunemaa T, Biegalski S, Landsberger S, Maenhaut W, Artaxo P, Cohen D (1997) Characterization of the gent stacked filter unit PM10 sampler. Aerosol Sci Technol 27(6):726–735. https://doi.org/10.1080/02786829708965507

Janjani H, Nabizadeh R, Shamsipour M, Yunesian (2020) Association between exposure to ambient fine particulate matter and prevalence of type 2 diabetes in Iran: an ecological study. Environ Sci Pollut Res 27:26182–26190. https://doi.org/10.1007/s11356-020-08659-7

Kerminen VM, Ojanen C, Pakkanen T, Hillamo R, Aurela M, Merilainen J (2000) Low-molecular weight dicarboxylic acids in an urban and rural atmosphere. J Aerosol Sci 31:349–362. https://doi.org/10.1016/S0021-8502(99)00063-4

Keuken MP, Moerman M, Voogt M, Blom M, Weijers EP, Röckmann T, Dusek U (2013) Source contributions to PM2.5 and PM10 at an urban background and a street location. Atmos Environ 71:26–35. https://doi.org/10.1016/j.atmosenv.2013.01.032

Kim D, Chen Z, Zhou L-F, Huang S-X (2018) Air pollutants and early origins of respiratory diseases. Chron Dis Translat Med 4:75e94. https://doi.org/10.1016/j.cdtm.2018.03.003

Klopper D, Formenti P, Namwoonde A, Cazaunau M, Chevaillier S, Feron A, Gaimoz C, Hease P, Lahmidi F, Mirande-Bret C, Triquet S, Zeng Z, Piketh SJ (2020) Chemical composition and source apportionment of atmospheric aerosols on the Namibian coast. Atmos Chem Phys 20:15811–15833. https://doi.org/10.5194/acp-20-15811-2020

Kušan AC, Kroflič A, Grgić I, Ciglenečki I, Frka S (2020) Chemical characterization of fine aerosols in respect to water-soluble ions at the eastern Middle Adriatic coast. Environ Sci Pollut Res 27:10249–10264. https://doi.org/10.1007/s11356-020-07617-7

Maenhaut W, Francois F, Cafmeyer J (1994) The Gent Stacked Filter Unit (SFU) sampler for the collection of atmospheric aerosols in two size fractions: description and instructions for installation and use. NAHRES-19:249-263.https://inis.iaea.org/collection/NCLCollectionStore/_Public/25/054/25054927.pdf. Accessed 24 April 2020

Mason B, Moore CB (1982) Principles of geochemistry, 4th edn. Wiley, New York

Micic S, Shang JQ, Lo KY (2003) Improvement of the load-carrying capacity of offshore skirted foundations by electrokinetics. Can Geotech J 40:949–963. https://doi.org/10.1139/t03-045

Mico S, Tsaousi E, Deda A, Pomonis P (2015) Characterization of airborne particles and source identification using SEM/EDS. Eur Chem Bull 4(4):224–229. https://doi.org/10.17628/ecb.2015.4.224-229

Miranda RM, Andrade MF, Fornaro A, Astolfo R, Andre PA, Saldiva P (2012) Urban air pollution: a representative survey of PM2.5 mass concentrations in six Brazilian cities. Air Qual Atmos Health 5:63–77. https://doi.org/10.1007/s11869-010-0124-1

Moallemi A, Kazemimanesh M, Corbin JC, Thomson K, Smallwood G, Olfert JS, Lobo P (2019) Characterization of black carbon particles generated by a propane-fueled miniature inverted soot generator. J Aerosol Sci 135:46–57. https://doi.org/10.1016/j.jaerosci.2019.05.004

Moore E, Chatzidiakou L, Kuku M-O, Jones RL, Smeeth L, Beevers S, Kelly FJ, Barratt B, Quint JK (2016) Global associations between air pollutants and chronic obstructive pulmonary disease hospitalizations—a systematic review. Ann Am Thorac Soc 13(10):1814–1827. https://doi.org/10.1513/AnnalsATS.201601-064OC

Mouli PC, Mohan SV, Reddy SJ (2003) The study on major inorganic ion composition of atmospheric aerosols at Tirupati. J Hazard Mater B 96:217–228

Myhre G, Myhre CEL, Samset BH, Storelvmo T (2013) Aerosols and their relation to global climate and climate sensitivity. Nature Edu Knowl 4(5):7

NOAA- National Oceanic and Atmospheric Administration (2019) http://ready.arl.noaa.gov/HYSPLIT.php Acessed: January, 2019

Oliveira C, Martins N, Tavares J, Pio C, Cerqueira M, Matos M, Silva H, Oliveira C, Camões F (2011) Size distribution of polycyclic aromatic hydrocarbons in a roadway tunnel in Lisbon, Portugal. Chemosphere 83:1588–1596. https://doi.org/10.1016/j.chemosphere.2011.01.011

Polichetti G, Cocco S, Spinali A, Trimarco V, Nunziata A (2009) Effects of particulate matter (PM_{10}, $PM_{2.5}$ and PM_1) on the cardiovascular system- rewiew. Toxicology 261:1–8. https://doi.org/10.1016/j.tox.2009.04.035

Pósfai M, Simonics R, Li J, Hobbs PV, Buseck PR (2003) Individual aerosol particles from biomass burning in southern Africa: compositions and size distributions of carbonaceous particles. J Geophys Res 108:8483. https://doi.org/10.1029/2002JD002291

Reis MA, Carvalho A, Taborda A, Quaresma A, Dias G, Alves LC, Mota M, Chaves PC, Teixeira R, Rodrigues PO (2009) High airborne PM2.5 chlorine concentrations link to diabetes surge in Portugal. Sci Total Environ 407:5726–5734. https://doi.org/10.1016/j.scitotenv.2009.07.029

Riant M, Meirhaeghe A, Giovannelli J, Occelli F, Havet A, Cuny D, Amouyel P, Dauchet L (2018) Associations between long-term exposure to air pollution, glycosylated hemoglobin, fasting blood glucose and diabetes mellitus in northern France. Environ Int 120:121–129. https://doi.org/10.1016/j.envint.2018.07.034

Rolph G, Stein A, Stunder B (2017) Real-time environmental applications and display system: READY. Environ Model Softw 95:210–228. https://doi.org/10.1016/j.envsoft.2017.06.025

Satsangi PG, Yadav S (2014) Characterization of PM2.5 by X-ray diffraction and scanning electron microscopy–energy dispersive spectrometer: its relation with different pollution sources. Int J Environ Sci Technol 11:217–232. https://doi.org/10.1007/s13762-012-0173-0

Seinfeld JH, Pannis SN (1998) Atmospheric chemistry and physics – from air pollution to climate change. Wiley, N.Y.

Silva FS, Godoi RHM, Tauler R, André PA, Saldiva PHN, van Grieken R, Marchi MRR (2015) Elemental composition of PM2.5 in Araraquara City (Southeast Brazil) during seasons with and without sugar cane burning. J Environ Prot 6(6):426–434. https://doi.org/10.4236/jep.2015.65041

Soleimani M, Amini N, Sadeghian B, Wang D, Fang L (2018) Heavy metals and their source identification in particulate matter (PM 2.5) in Isfahan City, Iran. J Environ Sci 72:166–175. https://doi.org/10.1016/j.jes.2018.01.002

Statistica (2007) Data analysis software system, version 8.0. StatSoft, Inc. ww.statsoft.com

Strzelec M, Proemse BC, Barmuta LA, Gault-Ringold M, Desservettaz M, Boyd PW, Perron MMG, Schofield R, Bowie AR (2020) Atmospheric trace metal deposition from natural and anthropogenic

sources in Western Australia. Atmosphere 11:474–501. https://doi.org/10.3390/atmos11050474
Sutton MSR, Riddick SN, Dragosits U, Nemitz E, Theobald MR, Tang YS, Braban CF, Vieno M, Dore AJ, Mitchell RF, Wanless S, Daunt F, Fowler D, Blackall TD, Milford C, Flechard CR, Loubet B, Massad R, Cellier P, Personne E, Coheur PF, Clarisse L, Damme MV, Ngadi Y, Clerbaux C, Skjøth CA, Geels C, Hertel O, Kruit RJW, Pinder RW, Bash JO, Walker JT, Simpson D, Horváth L, Misselbrook TH, Bleeker A, Dentener F, Vries W (2013) Towards a climate-dependent paradigm of ammonia emission and deposition. Philos Trans R Soc B Biol Sci 368:1–13. https://doi.org/10.1098/rstb.2013.0166
Tian Y, Xiang X, Wu Y, Cao Y, Song J, Sun K, Liu H, Hu Y (2017) Fine particulate air pollution and first hospital admissions for ischemic stroke in Beijing, China. Sci Rep 7(1):3897. https://doi.org/10.1038/s41598-017-04312-5
Twomey S (1977) Influence of pollution on shortwave albedo of clouds. J Atmos Sci 34:1149–1152
U.S. EPA (2018). Volatile organic compounds emissions (Report on the Environment, 2018). https://cfpub.epa.gov/roe/indicator_pdf. Acessed: June 2020.
UN (2018) https://population.un.org/wup/Publications/Files/WUP2018-PopFacts_2018-1.pdf, accessed: January, 2020
Urbančok D, Payne AJR, Webster RD (2017) Regional transport, source apportionment and health impact of PM10 bound polycyclic aromatic hydrocarbons in Singapore's atmosphere. Environ Pollut 229: 984–993. https://doi.org/10.1016/j.envpol.2017.07.086
Vu TV, Delgado-Saborit JM, Harrison RM (2015) Review: Particle number size distributions from seven major sources and implications for source apportionment studies. Atmos Environ 122:114–132. https://doi.org/10.1016/j.atmosenv.2015.09.027
West GH, Cooper MR, Burrelli LG, Dresser D, Lippy BE (2018) Exposure to airborne nano-titanium dioxide during airless spray painting and sanding. J Occup Environ Hyg 16(3):218–228. https://doi.org/10.1080/15459624.2018.1550295
WHO - World Health Organization. (2006) Air quality guidelines for particulate matter, ozone, nitrogen dioxide and sulfur dioxide: global update 2005: summary of risk assessment. https://www.who.int/phe/health_topics/outdoorair/outdoorair_aqg/en/. Accessed: March 2020.
Wiedensohler A, Andrade M, Weinhold K, Müller T, Birmili W, Velarde F, Moreno I, Forno R, Sanchez MF, Laj P, Ginot P, Whiteman DN, Krejci R, Sellegr K, Reichler T (2018) Black carbon emission and transport mechanisms to the free troposphere at the La Paz/El Alto (Bolivia) metropolitan area based on the Day of Census (2012). Atmos Environ 194:158–169. https://doi.org/10.1016/j.atmosenv.2018.09.032
Yao XH, Fang M, Chan CK, Ho KF, Lee SC (2004) Characterization of dicarboxylic acids in PM2.5 in Hong Kong. Atmos Environ 38:963–970. https://doi.org/10.1016/j.atmosenv.2003.10.048
Zheng X-Y, Ding H, Jiang L-N, Chen S-W, Zheng J-P, Qiu M, Zhou Y-X, Chen Q, Guan W-J (2015) Association between air pollutants and asthma emergency room visits and hospital admissions in time series studies: a systematic review and meta-analysis. PLoS ONE 18: e0138146. https://doi.org/10.1371/journal.pone.0138146